Sensors & Actuators: A. Physical 399 (2026) 117446

Contents lists available at ScienceDirect

Sensors and Actuators: A. Physical

journal homepage: www.journals.elsevier.com/sensors-and-actuators-a-physical

Electrical and thermo-mechanical properties of styrene-ethylene-butylene-styrene/carbon nanotube and styrene-ethylene-butylene-styrene/carbon black multipin electrodes for electroencephalography

George Gnonhoue *, Ilyass Tabiai *, Jérémie Voix, Éric David

Université du Québec, École de technologie supérieure, 1100 Notre-Dame Street West, Montreal, Quebec H3C 1K3, Canada

ARTICLE INFO

Keywords:
Flexible EEG electrodes
Electrical conductivity
Contact impedance
Signal quality
Multipin electrodes
Wearable neurotechnology

ABSTRACT

Flexible electroencephalography (EEG) electrodes have attracted increasing attention due to their potential applications in mobile health monitoring. However, balancing electrical conductivity, flexibility, stretchability, and EEG signal recording remains challenging. Here, we fabricated polystyrene-block-poly(ethylene butylene)-block-polystyrene (SEBS) composites with carbon nanotubes (CNT) and carbon black (CB) via solvent dissolution. The percolation threshold was approximately 12 wt% for SEBS/CB composites and approximately 2 wt% for SEBS/CNT composites. At 20 wt%, SEBS/CB composite conductivity plateaued at 0.01 S/m, whereas SEBS/CNT composite conductivity reached 1.26 S/m at 16 wt%. Contact impedance was 4.2 ± 0.45 kΩ for SEBS/16 wt% CNT and 5.4 ± 0.9 kΩ for SEBS/20 wt%CB. SEBS/CNT was slightly stiffer than SEBS/CB. The electrodes reliably recorded EEG signals, demonstrating their potential for health monitoring and long-term EEG measurements.

1. Introduction

The development of wearable electronics has transformed electroencephalogram (EEG) electrode technology [1–3]. EEG electrodes are sensors that detect brain activity, and traditional EEG systems typically employ rigid, wet electrodes with conductive gel to ensure stable contact and low impedance at the skin-electrode interface However, wet electrodes can be uncomfortable, cause skin irritation or hair damage with prolonged use, and necessitate application by skilled personnel, who may perform skin abrasion to optimize contact impedance [4]. The conductive gel dries out, limiting measurement duration and impacting signal quality, making gel-based EEG systems less than ideal for non-laboratory settings [5–7].

To address the limitations associated with wet electrodes, semi-dry electrodes have recently emerged as a promising alternative. These systems deliver a minimal amount of electrolyte to the scalp via porous or absorbent media, forming a hydrated interface that effectively stabilizes contact impedance. Despite their advantages, electrolyte-based interfaces, including semi-dry configurations, still pose a risk of skin irritation or infection [8]. Moreover, semi-dry electrode technology continues to face technical challenges such as precise control over electrolyte release [9], prevention of short circuits between neighboring electrodes, and maintaining structural integrity under mechanical pressure during use [10]. Recent advances have highlighted the potential of hydrogel-based materials to support controlled electrolyte release in semi-dry configurations. In particular, flexible hydrogels such as polyvinyl alcohol/polyacrylamide (PVA/PAM) and Fe^{3+}-doped gelatin/poly(acrylate-co-acrylamide) have demonstrated acceptable electrochemical properties, with contact impedance values of 18 ± 8.9 kΩ and 17.8 ± 3.69 kΩ at 10 Hz, respectively [11,12]. These materials exhibit strong signal correlation with conventional wet electrodes during standard EEG paradigms (eyes closed/open) and ensure better moisture retention, mechanical resilience, and long-term comfort. Studies [13,14] emphasize that semi-dry electrodes combine the mechanical flexibility of dry systems with the signal stability of wet electrodes, making them suitable for continuous, high-fidelity EEG monitoring in wearable and brain-computer interface applications. The high conductivity of the electrodes enabled reliable acquisition of cortical electrical activity, essential for exploring complex cognitive processes and higher-order consciousness. In this context, the recent work by Sidheekha *et al.* [15] provides valuable insights into multifunctional conductive polymer-based electrodes. They introduced

* Corresponding authors.
E-mail addresses: olatoundji-george.gnonhoue.1@ens.etsmtl.ca (G. Gnonhoue), Ilyass.Tabiai@etsmtl.ca (I. Tabiai).

https://doi.org/10.1016/j.sna.2025.117446
Received 22 May 2025; Received in revised form 25 December 2025; Accepted 29 December 2025
Available online 30 December 2025

polyaniline/chitosan (PANI/CS) hybrid hydrogels that act as both energy storage devices and self-sensing elements. These electrodes utilize the redox-driven faradaic properties of polyaniline to detect variations in current, temperature, and electrolyte concentration through changes in potential and energy consumption. This integrated sensing-storage approach, requiring no additional connectivity, highlights the potential of conductive polymer composites for next-generation bioelectronic interfaces.

Despite their advantages, semi-dry electrodes are not a definitive solution. Their reliance on hydrated interfaces introduces limitations such as electrolyte evaporation, limited shelf life, and potential material degradation. Furthermore, skin irritation risks, manufacturing complexity, and maintenance requirements may hinder their widespread adoption for daily or long-term EEG monitoring. These drawbacks have sustained interest in the development of fully dry electrodes, which aim to simplify use while maintaining high signal fidelity and comfort. This work focuses on designing dry and flexible EEG electrodes based on Polystyrene-block-poly(ethylene butylene)-block polystyrene (SEBS) and carbon-based conductive fillers. These electrodes are a gel-free, user-friendly alternative that maintains stable performance over hair-covered regions, addressing challenges in wearable neurotechnology.

Recent efforts have focused on next-generation EEG systems that eliminate the need for any gel or liquid interface. Dry electrodes, especially those based on flexible materials, provide stable contact with the skin's curved surface, unlike rigid electrodes, which do not conform to scalp contours and limit EEG signal acquisition [7,16,17]. Consequently, recent studies have been exploring flexible, multifunctional composite materials to enhance EEG electrode performance and user comfort [7, 18]. Multifunctional composite materials are being developed to create EEG electrodes with optimal flexibility, conductivity, and comfort for long-term use [19–23]. Ergonomic, flexible multipin geometries have improved EEG signal quality and user comfort, enhancing the potential for diagnostics and neuroscience research [24–34]. Thermoplastic polyurethane (TPU) and polydimethylsiloxane (PDMS), combined with carbon reinforcements, show promise for fabricating flexible electrodes [35–37]. Carbon black (CB) and carbon nanotubes (CNTs) are commonly incorporated into polyurethane (PU) and PDMS to produce multipin EEG electrodes [25,38–42]. These materials achieve electrical conductivity through a conductive surface coating or by embedding carbon reinforcements to enhance volume conductivity, enabling stable signal acquisition in dry conditions. Fiedler *et al.* [43] developed a 24-pin dry EEG electrode made of polyurethane and coated with Ag/AgCl for ergonomic and flexible multipin EEG electrodes. Integrated into a textile cap, the system can accommodate up to 97 multipin electrodes. In tests comparing this 97-channel dry EEG cap with a conventional 128-channel wet EEG cap, parameters such as resting-state EEG, alpha activity, eye blinks, and visual evoked potentials were evaluated. The wet electrodes-maintained impedance values below 20 kΩ, while the dry electrodes exhibited average impedances below 150 kΩ for 92 of the 97 channels. Despite the higher impedance, the system reliably recorded EEG signals. Heijs *et al.* [31] also validated flexible multipin dry electrodes against a commercial wet system. Their dry electrode setup consisted of 32 AgCl-coated polyurethane electrodes fabricated via electroless plating, whereas the wet system employed 32 Ag/AgCl gel electrodes. EEG signal acquisition was evaluated using auditory stimuli and tasks involving eyes-open and eyes-closed conditions. The mean impedance of the wet electrodes was 6.8 ± 5.6 kΩ, whereas the dry electrodes exhibited a higher mean impedance of 602 ± 401 kΩ. Wand *et al.* [44] designed a dry, claw-shaped EEG electrode for detecting signals in both hairy and non-hairy areas. This electrode, fabricated entirely from 3D-printed TPU, features a conductive coating created by blending TPU with a silver (Ag) solution. Its performance was evaluated against that of a traditional wet electrode through contact impedance tests and EEG signal acquisition during tasks involving eye-opening and eye-closing conditions. The wet electrode exhibited contact impedance values of 5 kΩ at 1 Hz in hairless areas and 10 kΩ in hairy areas, while the TPU electrode exhibited higher impedances of 18.6 kΩ and 122 kΩ in hairless and hairy regions, respectively. Xing and Casson [45] also developed flexible, 3D-printed TPU multipin electrodes, which exhibited a typical contact impedance in the 100–200 kΩ range, demonstrating their suitability for flexible electrodes with moderate impedance for EEG signal capture.

Recent studies have explored PDMS and innovative designs for flexible, long-wear EEG electrodes to enhance user comfort and signal reliability in both hairy and non-hairy scalp areas. Das *et al.* [46] developed electrodes that combine CNT, PDMS, and graphene, highlighting the affordability, biocompatibility, and robustness of graphene. These electrodes performed comparably to traditional silver/silver chloride (Ag/AgCl) electrodes. Oh *et al.* [47] fabricated multi-walled carbon nanotube (MWCNT) and PDMS composites using paste mixing and three-roll milling, producing a series of composites with varying CNT content (0.5–10 wt%). As CNT concentration increased, the conductivity of the composite rose, peaking at 100 S/m beyond 5 wt%. The contact impedance of these composites was evaluated, with wrinkled electrodes achieving 19 kΩ and unwrinkled electrodes achieving 38 kΩ at 1 kHz. These electrodes were validated with eye movement and cognitive tasks. Sharma *et al.* [48], prepared MWCNT-PDMS composites using a solution-based method, creating electrodes with an impedance comparable to that of silver/silver chloride (Ag/AgCl) across the 20 Hz–1 kHz spectrum. For example, MWCNT-PDMS dry electrodes exhibited an impedance ranging from 626 kΩ at 20 Hz to 124 kΩ at 1 kHz, closely matching that of silver/silver chloride (Ag/AgCl) electrodes. Wang *et al.* [49] designed flexible PDMS-based multipin dry electrodes coated with a gold layer and fabricated using manual and ultrasonic methods. These electrodes, having either 13 or 21 pins, recorded EEG signals effectively through hair without the use of conductive gel. In non-hairy areas, the silicone dry electrodes exhibited impedance levels of 8.0 kΩ at 20 Hz and 5.0 kΩ at 10 kHz without skin preparation, while in hairy areas, they yielded 18 kΩ at 20 Hz and 10 kΩ at 10 kHz. Stability testing over 5.5 h revealed that the dry electrodes maintained a consistent impedance of around 3.8 kΩ, while those of the wet electrodes increased from an initial 1.8 kΩ to over 8 kΩ within the same period. EEG electrode technology has shifted toward dry, flexible, and user-friendly alternatives to rigid wet electrodes, which are often uncomfortable, complex to apply, and exhibit signal instability during prolonged use. Flexible polymers such as PDMS and TPU, combined with conductive fillers like carbon nanotubes (CNTs) and carbon black (CB), have demonstrated significant potential for the fabrication of multipin electrodes capable of maintaining reliable skin contact, including on hairy scalp regions. Despite these advantages, challenges remain, including high contact impedance, limited scalability of fabrication, and mechanical properties that may hinder long-term comfort and durability. Conductive polymer composites such as polystyrene-block-poly (ethylene butylene)-block-polystyrene (SEBS)/CB and SEBS/CNT are not restricted to EEG applications. Compared with conventional PDMS- and TPU-based flexible electrodes, SEBS/CB composites provide clear benefits in processing simplicity, cost, and scalability. SEBS is a thermoplastic elastomer that can be easily processed by melt-mixing, hot pressing, or extrusion without the need for curing or vacuum-degassing steps, allowing for swift production. [50,51]. Recent studies have demonstrated that SEBS-based materials can also be engineered into porous, breathable, and recyclable structures suitable for wearable and thermal-management applications while maintaining excellent flexibility and mechanical robustness [52–54]. Furthermore, both SEBS and carbon black are low-cost, recyclable materials that can be reprocessed using standard thermoplastic routes, providing a sustainable and environmentally friendly alternative for large-scale manufacturing of flexible EEG electrodes [55]. Their combination of electrical conductivity, mechanical softness, and long-term durability makes them promising for bioelectronic interfaces, including electrocardiography (ECG), electromyography (EMG), and other skin-mounted sensors. Nevertheless, EEG

electrodes impose more stringent functional requirements. They must ensure low contact impedance without conductive gel, maintain skin contact through hair-covered scalp regions, and provide stable signal acquisition over extended periods, even with micro-movements [56–59]. Meeting these challenges requires elastomeric materials that are conductive, compliant, biocompatible, and conform closely to the scalp's complex geometry [60]. SEBS-based composites are strong candidates for next-generation dry EEG electrodes and versatile for broader biomedical sensing platforms. SEBS, a thermoplastic elastomer known for its flexibility, softness, and skin compatibility, has attracted attention in piezoresistive sensors and ECG devices [20,61–67]. However, its application in EEG systems, particularly in composite configurations incorporating carbon nanotubes (CNTs) or CB, remains insufficiently explored. To address this gap, this study comparatively evaluates SEBS/CB and SEBS/CNT composites for flexible multipin EEG electrodes. This investigation builds on our previous comparative work with SEBS/CB and ethylene-vinyl acetate (EVA)/CB composites, which identified SEBS/CB as promising due to its superior electrical, mechanical, and stability properties. We extend that approach by integrating CNTs and systematically characterizing the composites' electrical performance (via impedance spectroscopy and conductivity), mechanical flexibility (via dynamic mechanical analysis), and thermal stability. This study does not aim to validate the electrodes in terms of EEG signal decoding or clinical performance. Instead, we focus on evaluating material properties critical for designing reliable, comfortable dry EEG electrodes. A dedicated clinical study assessing long-term recording quality and usability across multiple users and conditions is outside this paper's scope and will be considered in future work. The goal is to identify the composite material that best balances electrical conductivity, low contact impedance, mechanical compliance, thermal stability, and scalp conformity. Ultimately, this research aims to support the development of durable, high-performance EEG electrodes suitable for extended, real-world use.

2. Materials and methods

This section investigates the use of polystyrene-block-poly(ethylene butylene)-block polystyrene (SEBS)-based materials to enhance EEG measurements. It compares SEBS/carbon black and SEBS/CNT composites with a commercial dry flexible electrode to identify the formulation with superior electrical conductivity and lower contact impedance. This study does not evaluate clinical efficacy or brain-signal decoding performance. The focus is on assessing critical material properties—electrical behavior, mechanical compliance, and electrode-skin contact stability—that determine the suitability of these composites for flexible dry EEG electrodes. A follow-up clinical study involving long-term and multi-subject EEG recordings will be considered in future work.

2.1. Materials

Polystyrene-block-poly(ethylene butylene)-block polystyrene (SEBS), with a number average molecular weight of 54,000 g/mol and a polystyrene content of 30 wt%, was supplied by Kraton (Kraton, Paulínia – SP, Brazil). SEBS was selected as the base material for fabricating flexible EEG electrodes. Multiwalled Carbon Nanotubes (MWCNTs), specifically NC 7000™ from Nanocyl S.A. (Sambreville, Belgium), were used as conductive fillers. These nanotubes have an average diameter of 9.5 nm, an average length of 1.5 μm, a surface area of 250–300 m^2/g, a nominal electrical conductivity of 100 S/m, a density of 1.30–2.00 g/cm^3 , and a carbon purity of 90 %. Carbon Lampblack nanoparticles (C198–500, Lot 145509), purchased from Fisher Chemical (Fisher Scientific Company, Ottawa (ON), Canada), were also used. These particles have a diameter of 50 nm, a nominal conductivity of 400 S/m, and a density of 1.8 g/cm^3 . For the dissolution, UN1294 toluene Optima (T291–4, Lot 234238), also from Fisher Chemical, was used.

2.2. Electrode preparation

The composites were prepared by dissolving pure SEBS in toluene at a fixed solvent-to-polymer ratio of 10 mL g^{-1} (i.e., 100 mL of toluene for 10 g of total composite). Solvent blending was selected to achieve nanoscale dispersion of conductive fillers while preserving the anisotropic structure of carbon nanotubes, which is essential for efficient electrical percolation. When properly recovered, the solvent does not introduce environmental concerns and enables more uniform filler distribution and stable conductivity compared with dry mechanical mixing [68,69]. The dissolution was carried out at 100 °C under magnetic stirring at 600 rpm until a homogeneous polymer solution was obtained. Subsequently, carbon nanotubes (CNT, 0–16 wt%) and carbon black (CB, 0–25 wt%), as summarized in Table 1, were gradually added to the solution. The mixture was maintained under the same stirring conditions (600 rpm, 100 °C) for an additional 30 min to promote uniform filler dispersion and minimize agglomeration.

After casting, the mixture was placed under a fume hood and dried at room temperature for at least 24 h to ensure complete solvent evaporation. This extended drying period was chosen to facilitate the full removal of toluene before moulding. The resulting composite was molded by compression to manufacture multipin-shaped EEG electrodes at a temperature of 215 °C, with an initial pressure of 0.8 MPa for 5 min, followed by an increase to 5 MPa for an additional 15 min while maintaining the temperature. During the subsequent hot-pressing process used to form the multipin electrode geometry, the material was processed at 215°C, well above the boiling point of toluene (110°C), adding an extra thermal step for solvent removal. These combined ventilated drying and high-temperature moulding steps help reduce the chances of residual toluene in the final electrodes. Each electrode consisted of 19 pins, with each pin measuring 4.9 ± 0.09 mm in height and 1.41 ± 0.01 mm in diameter. The pins were arranged in a circular configuration with a center-to-center spacing of approximately 2.5 mm, resulting in an inter-electrode edge-to-edge spacing of approximately 1.1 mm on the contact surface. This multipin layout is designed to improve contact performance on hairy scalp regions by allowing the pins to gently part the hair and establish multiple low-impedance contact points on the skin. This configuration enhances signal quality and reduces motion artifacts during EEG acquisition.

The nanocomposites fabricated using this procedure are listed in Table 1. Three samples of each nanocomposite were used for characterization.

2.3. Methods

2.3.1. Electrical characterization

Electrical characterization assesses the electrical performance and conductivity of composite electrodes, crucial for EEG signal acquisition with minimal distortion. The electrical conductivities of the composites were measured using a frequency-domain broadband dielectric spectrometer (BDS) (Alpha-A Dielectric Analyzer, Novocontrol, Germany).

Table 1
SEBS/CNT and SEBS/CB nanocomposites at different carbon nanoparticle weight fractions.

SEBS/CNT		SEBS/CB	
Reinforcements (wt%)	Matrix (wt%)	Reinforcements (wt%)	Matrix (wt%)
0	100	0	100
4	96	5	95
6	94	10	90
8	92	12	88
10	90	15	85
12	88	20	80
14	86	25	75
16	84	-	

Circular samples with a diameter of 20 mm and a thickness of 1.2 mm were mounted between two solid brass electrodes, forming a typical plane-plane electrode/composite/electrode sandwich configuration. Measurements were performed from 10^{-2} Hz to 10^{5} Hz at 30°C. This setup accurately determines complex impedance, providing insights into the material's conductive behavior, frequency-dependent response, and electrochemical stability—critical parameters for high-performance EEG electrodes.

2.3.2. Structural characterization

Structural characterization examines the composite's internal morphology and evaluates the dispersion of conductive particles within the polymer matrix, factors influencing electrical performance and mechanical integrity. We used a high-resolution scanning electron microscope (SEM) (Hitachi SU-8230 field emission) at an accelerating voltage of 5 kV. To prepare the samples, composite cross-sections were obtained via cryogenic sectioning to preserve the internal structure. These cross-sections were coated with a ~2 nm layer of platinum under vacuum using a turbo-pumped sputter/carbon coater (Q150T) to enhance surface conductivity and image resolution. This technique enables high-contrast imaging of the conductive filler network and assesses dispersion homogeneity, impacting the composite's functional properties.

2.3.3. Thermo-mechanical characterization

Thermo-mechanical characterization confirms conductive particle weight fractions, assesses thermal stability via decomposition temperatures, and evaluates mechanical behavior as a function of temperature. These properties are essential for material integrity during processing and use in biomedical applications such as EEG acquisition. To assess the thermal stability and validate the filler content, thermogravimetric analysis (TGA) was performed using a Diamond TG/differential thermal analysis (DTA) instrument (Perkin Elmer). Samples weighing approximately 10–13 mg were heated from 20°C to 500°C at a rate of 3 °C/min under a nitrogen atmosphere flowing at 100 mL/min. The temperature was held at 500°C for 2 min to ensure complete decomposition. This technique determines the decomposition onset, residual mass (used to verify the filler content), and the composites' thermal degradation profiles. To investigate the viscoelastic behavior of the composites, dynamic mechanical thermal analysis (DMTA) was conducted using a DMTA Q800 (TA Instruments Inc.). Tests were performed on polystyrene-block-poly(ethylene butylene)-block polystyrene (SEBS) and nanocomposites containing 16 wt% CNT and 20 wt% CB. A double cantilever clamp with a 22 mm frame size and a 2 mm center clamp was used. Rectangular specimens (8 mm width × 2 mm thickness) were tested at a constant strain of 0.4 %, a frequency of 1 Hz, and a heating rate of 2 °C/min over the 25 °C to 35 °C temperature range. All measurements were carried out under ambient laboratory conditions, with a temperature of approximately 23 °C and relative humidity of 45–55 %. Only the storage modulus was measured, providing insights into the stiffness and elastic behavior of the composites across the tested temperature range.

2.3.4. Preliminary in vivo validation

Preliminary in vivo validation was performed to assess the real-world performance of the developed flexible multipin EEG electrodes in terms of contact impedance and EEG signal acquisition quality. To reflect realistic application conditions, measurements were performed on hairy regions of the scalp. This step is crucial for determining their effectiveness and comfort compared to commercial solutions. Flexible multipin EEG electrodes were selected to evaluate contact impedance and EEG artifacts associated with eye blink reflex. These artifacts were wirelessly recorded using the OpenBCI™ 16-channel Cyton Biosensing Board (OpenBCI, New York (NY), USA) coupled with the Ultracortex 'Mark IV' electroencephalogram headset (OpenBCI, New York (NY), USA). Contact impedance was measured at 31 Hz using the same acquisition system, as illustrated in Fig. 1. To simulate conditions for wearable EEG applications, the skin was neither cleaned nor abraded before measurements. The electrodes were securely inserted into the headset, which was comfortably positioned on the subject's head without applying pressure to the electrode surfaces, ensuring a user-friendly testing environment. Commercial dry flexible electrodes from OpenBCI were used as references at positions 1, 2, and 5 on the headset, and the flexible multipin electrodes developed in this work were inserted at positions 3 and 4. Fig. 2 displays both the developed electrode and the commercial reference for visual comparison. Performance was evaluated by measuring contact impedance and EEG signal amplitude for both the developed electrodes and reference electrodes. For statistical reliability, three measurements were performed for each configuration, and the mean and standard deviation were calculated to quantify variability and repeatability. This in vivo validation provides insights into electrode-skin interface quality, signal integrity, and usability, and compares the developed and commercial EEG electrodes under real-world conditions.

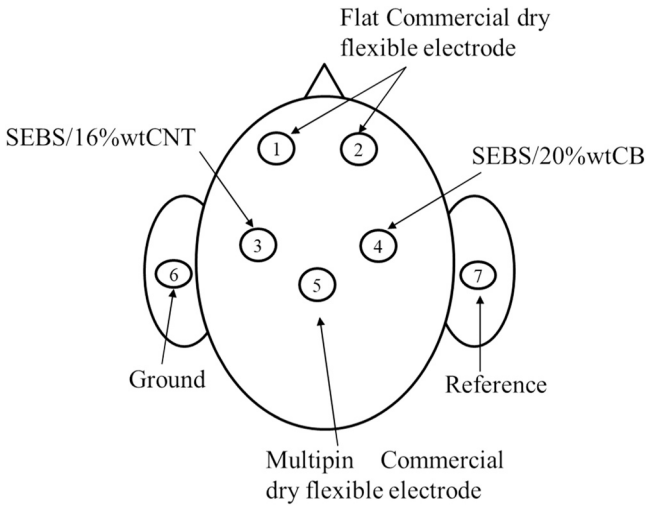

Fig. 1. Ultracortex "Mark IV" electroencephalography (EEG) headset for electrode placement. The headset ensures consistent and accurate positioning of EEG electrodes on the scalp to facilitate reliable EEG data acquisition.

2.3.5. Participants

Participant testing validated the effectiveness of the developed EEG electrodes under physiological conditions by assessing EEG signal quality and motion artifacts. Healthy adult participants (n = 4; 1 male and 3 females, aged between 21 and 35 years) were recruited for EEG measurements. All procedures were approved by the ÉTS Internal Review Board (Approval No. H20230504) and conducted according to the Declaration of Helsinki. Informed consent was obtained from all participants prior to the experiments. To ensure a controlled environment, participants were comfortably seated in a quiet room during signal acquisition. EEG signals were recorded for 10 s. Following standard EEG protocols and the American Clinical Neurophysiology Society guidelines [70], participants minimized head and facial muscle contractions and remained still to minimize motion artifacts. At a designated moment, participants were asked to blink in response to a sound cue in order to assess the ability of the electrodes to capture characteristic blink-related EEG activity.

3. Results

3.1. Electrical properties

Fig. 3 depicts the real part of the complex conductivity of polystyrene-block-poly(ethylene butylene)-block-polystyrene (SEBS)/carbon nanotube (CNT) and SEBS/carbon black (CB) composites as a

Fig. 2. Electroencephalography (EEG) electrode placement and signal acquisition using the 10–20 system. EEG measures electrical activity reflecting neuronal activity related to cognitive processes.

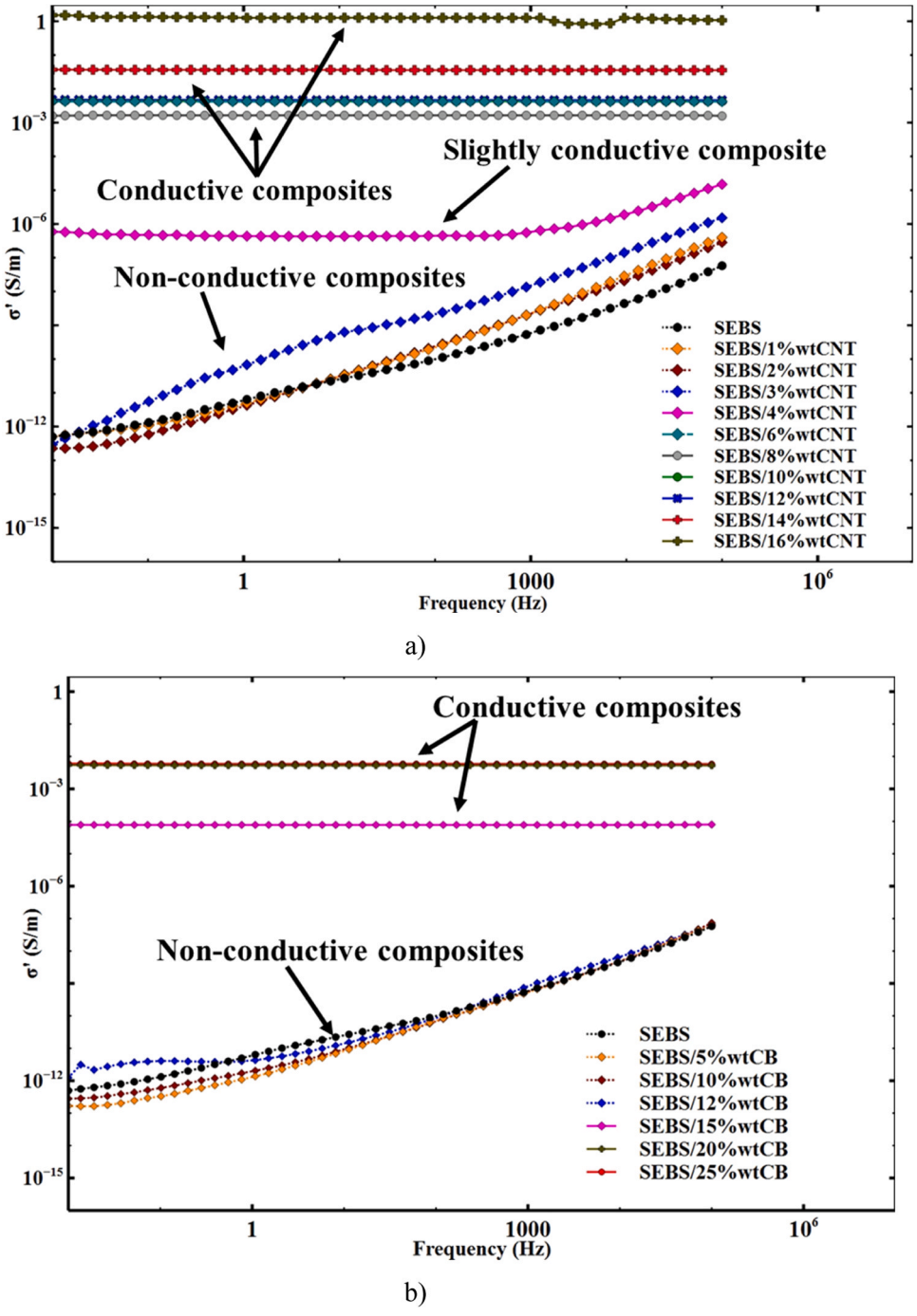

Fig. 3. Real part of the complex conductivity as a function of frequency of (a) SEBS/CNT and (b) SEBS/CB.

function of frequency. Above the percolation threshold, this value approximates the true direct current (DC) conductivity, and below this threshold, it overestimates conductivity because of a frequency-dependent term. As shown in Fig. 3, once the mass fraction of the composites exceeds 2 wt% of CNT and 12 wt% of CB, which are the respective percolation thresholds of SEBS/CNT and SEBS/CB composites, the electrical conductivity of the composites becomes independent of frequency. The variation in the real part of the complex conductivity of a composite material as a function of the concentration of the conductive filler can be divided into three regions. In the insulating region, at low conductive particle contents, the complex or AC conductivity is a function of frequency. This behavior is visible in Fig. 3 for concentrations below 12 wt%CB for the SEBS/CB composite and below 3 wt%CNT for the SEBS/CNT composite. With further increases in CB and CNT loading, the electrical conductivity becomes almost independent of frequency, and at this point, the composite material can be considered electrically conductive [71]. Fig. 3 also shows the non-conductive domain (0–12 wt% for SEBS/CB and 0–2 wt% for SEBS/CNT) that the value of the electrical conductivity at a given frequency is not monotonically correlated with the CB and CNT concentrations due to the contribution of the relaxation mechanisms. SEBS/20 wt%CB and SEBS/16 wt%CNT were chosen for the fabrication of the multipin electrodes to be used to perform the EEG measurements since they exhibit the highest electrical conductivities. The dotted curves in Fig. 3 represent the non-conductive composites, while the solid lines represent the conductive ones.

For SEBS/CNT composites:

- ❖ Conductivity increases with the CNT content.
- ❖ The percolation threshold occurs around 3–4 wt% of CNT.

Composites containing $\geq$ 6 wt% CNT as reinforcement exhibited stable electrical conductivity across a wide frequency range.

For SEBS/CB composites:

- ❖ Conductivity increases with the CB content.
- ❖ The percolation threshold occurs around 12–15 wt%of CB.
- ❖ Only composites containing $\geq$ 20 wt% CB exhibited high and stable electrical conductivity.

Fig. 4 shows the real part of the complex electrical conductivity of SEBS/CB and SEBS/CNT composites as a function of mass fraction at 1 Hz. The percolation thresholds for SEBS/CB and SEBS/CNT composites were approximately 12 wt% and 2 wt%, respectively. In Fig. 4, it can be observed that beyond the percolation threshold, the electrical conductivity of SEBS/CB composites reached a plateau at 0.01 S/m at 20 wt%, while that of the SEBS/CNT composite is 1.26 S/m at 16 wt%. Fig. 4 shows that the percolation threshold of SEBS/CNT composites is lower than that of SEBS/CB. At a mass fraction of 2 wt% of CNT within the matrix, SEBS/CNT composites begin to exhibit electrical conductivity, while the SEBS/CB counterparts start to be electrically conductive at a mass fraction of 12 wt% of CB.

Increasing the mass fraction of conductive reinforcements significantly enhances the electrical conductivity of the composites. A distinct percolation threshold was observed at approximately 12 wt% for SEBS/CB and 2 wt% for SEBS/CNT, indicating the formation of continuous conductive networks at lower filler contents in the CNT-based composites. Beyond the percolation threshold, SEBS/CB composites exhibit conductivity stabilization near 20 wt% CB due to network saturation and particle aggregation, while SEBS/CNT composites maintain a steady conductivity increase owing to the superior dispersion and high aspect ratio of CNTs. This contrast highlights the greater efficiency of CNTs in forming continuous conductive networks and mitigating the percolation–saturation effect observed in CB-filled systems. This difference highlights the superior efficiency of CNTs in establishing conductive pathways as compared to carbon black.

3.2. *Structural properties*

Fig. 5 presents the SEM micrograph of polystyrene-block-poly (ethylene butylene)-block polystyrene (SEBS)/CNT composites containing 16 wt% and SEBS/CB composites containing 20 wt%CB. The results show that CNT particles appear to be well distributed in the polystyrene-block-poly(ethylene butylene)-block polystyrene (SEBS)/16 wt%CNT composites. Fig. 5(b) shows that some aggregates were

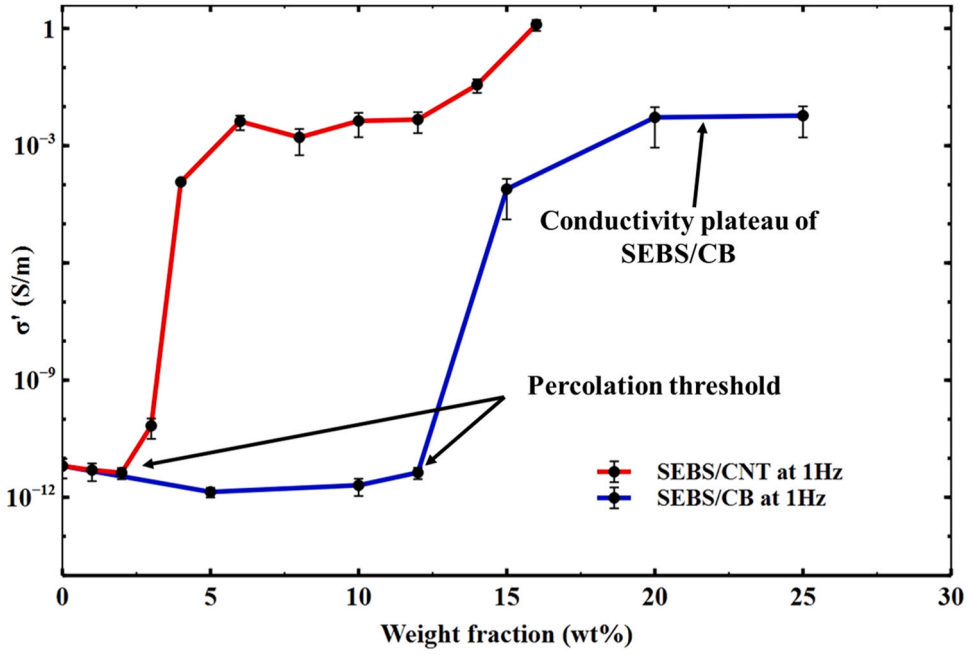

Fig. 4. Electrical conductivity of styrene-ethylene-butylene-styrene (SEBS) composites as a function of carbon nanotube (CNT) and carbon black (CB) filler loading (wt%).

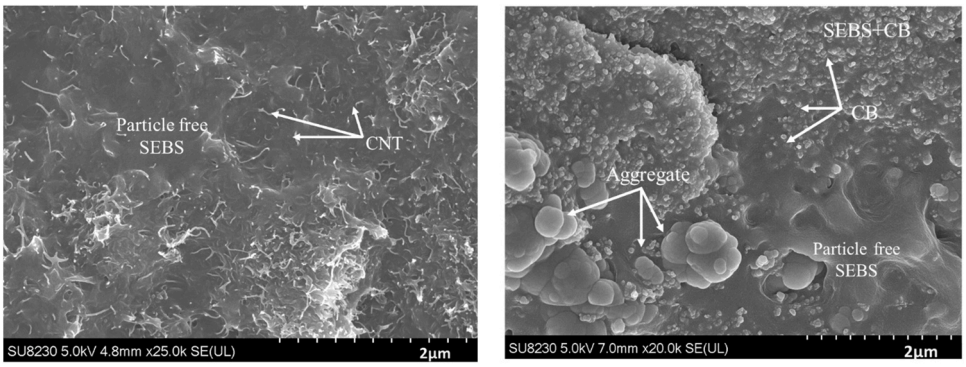

Fig. 5. Scanning electron microscopy (SEM) micrograph of a: (a) SEBS/16 wt%CNT composite and (b) SEBS/20 wt%CB composite.

observed in the SEBS/20 wt%CB composite due to the high concentration of CB (20 wt%). Fig. 5 illustrates the interaction of the reinforcing agents, CB and CNT, within the different matrices. The morphology of SEBS/16 wt%CNT composites revealed that, compared to SEBS/20 wt% CB, carbon black (CB) exhibited a greater aggregation in the matrix, whereas carbon nanotubes (CNTs) were more evenly distributed. A uniform dispersion of CB in SEBS may still pose challenges, especially at high concentrations. From an electrical properties standpoint, the presence of aggregates does not negatively impact the composite conductivity, as it facilitates the formation of conductive paths via CB-CB contacts [72–74]. Due to their geometric structure and large specific surface area, CNTs also promote CNT-CNT contacts within the SEBS/16 wt%CNT composite, enabling conductive pathways throughout the matrix.

3.3. Thermo-mechanical properties

A TGA was performed on the composites for which micrographic views were taken, as shown in Fig. 6. The TGA results compare the thermal stability and filler contents of SEBS/16 wt%CNT (red curve) and SEBS/20 wt% CB (blue curve). Both composites remain thermally stable with no significant weight loss in this range, indicating a good thermal resistance of the polymer-filler systems up to ~370°C. A sharp weight loss begins at around 370–400°C, corresponding to the thermal degradation of the SEBS matrix. The temperature at which decomposition starts is similar for both composites, suggesting a comparable thermal stability. After the complete degradation of the SEBS matrix (~500°C), the SEBS/20 wt%CB composite leaves about a 20 % residue, matching its carbon black content. The SEBS/16 wt%CNT composite leaves about a 16 % residue, consistent with its CNT content.

Fig. 7 presents a dynamic mechanical thermal analysis of neat polystyrene-block-poly(ethylene butylene)-block-polystyrene (SEBS), and SEBS/16 wt%CNT, and SEBS/20 wt%CB composites. It can be observed that the storage modulus of the SEBS/16 wt%CNT composite is higher than that of the SEBS/20 wt%CB composite, and that the storage modulus of pure SEBS is lower than those of the SEBS/16 wt%CNT and SEBS/2 wt%CB composites. It can be concluded that the presence of reinforcements within the matrices adds to the mechanical stiffness of the latter.

The addition of carbon nanotubes (CNTs) increases the storage modulus (E′) because CNTs reinforce the polymer matrix, increasing stiffness as compared to the pure polymer. The addition of CB to

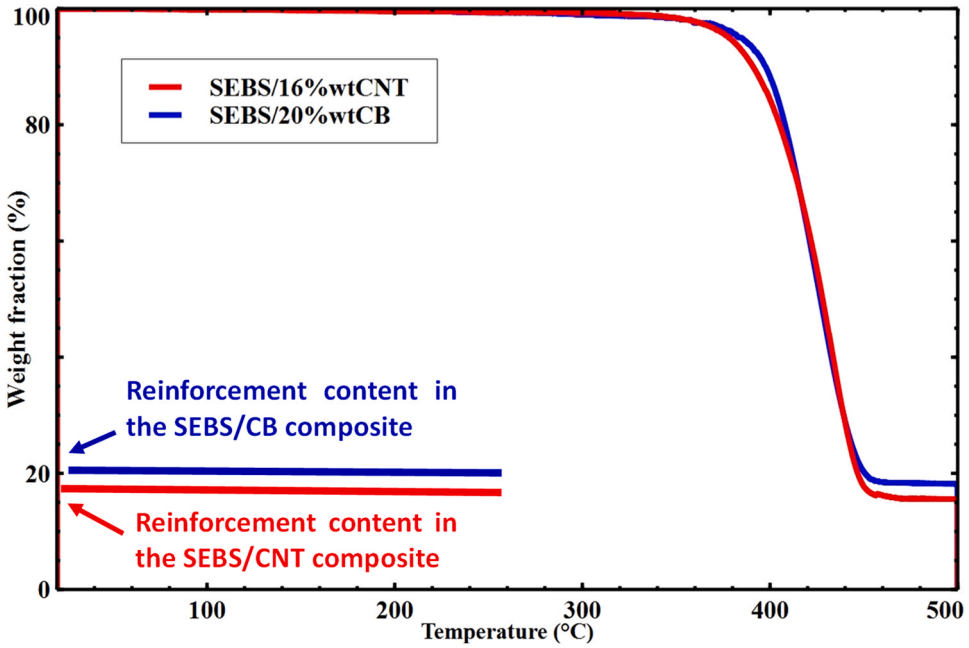

Fig. 6. TGA thermograms of SEBS/16 wt%CNT and SEBS/20 wt%CB.

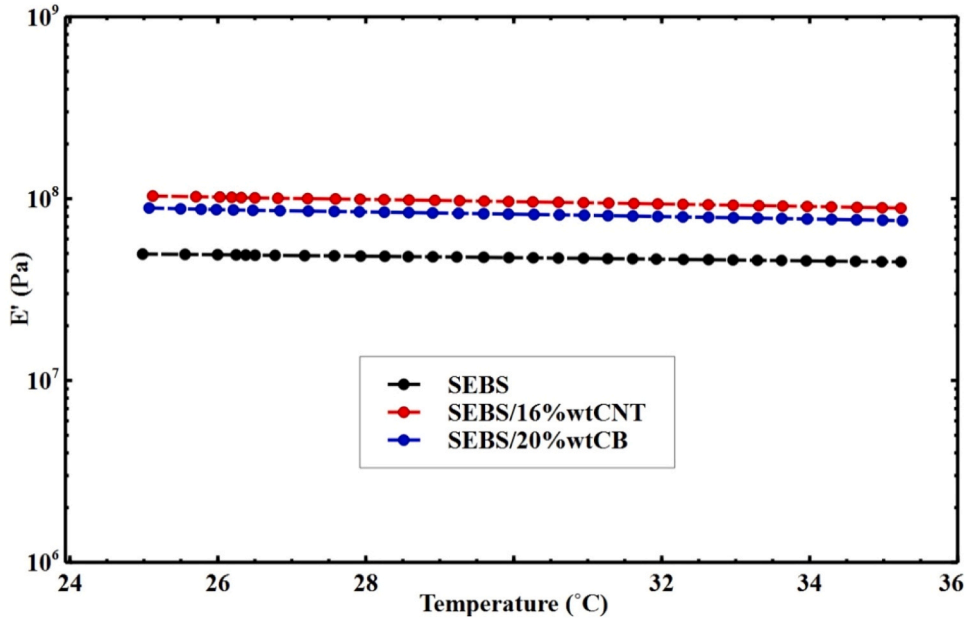

Fig. 7. DMTA thermograms of polystyrene-block-poly(ethylene butylene)-block polystyrene (SEBS) polymer, SEBS/carbon nanotube (CNT), and SEBS/carbon black (CB) composites.

polystyrene-block-poly(ethylene butylene)-block polystyrene (SEBS) also increases E′, but less so than CNTs, even at a loading of 20 %, which is in good agreement with the conductivity measurements.

3.4. *In vivo validation*

This section discusses the comparative analysis of the quality of multipin electrodes obtained from polystyrene- block- poly(ethylene butylene)- block- polystyrene (SEBS)/ 16 wt%CNT and SEBS/20 wt%CB composites versus commercial flexible electrodes at positions 1, 2, and 5, as presented in Fig. 1. The results provide insights into the performance of the various composites used in this work for EEG signal capture. Contact impedance is a key factor in EEG signal quality, varying with the electrode material. The higher electrical conductivity of the SEBS/16 wt%CNT composite as compared to the SEBS/20 wt%CB composite improved the quality of EEG signals by reducing the contact impedance between the electrode and the skin. The contact impedance reduction resulted in more stable signals, as shown in Fig. 8, under conditions of open and blinking eyes, where detecting subtle variations in the amplitude of EEG signals is important. The contact impedance of polystyrene-block-poly(ethylene butylene)-block polystyrene (SEBS)/ 16 wt% CNT electrodes with pins at position 3 is 4.2 ± 0.45 kΩ, as compared to commercial electrodes without pins at positions 1 and 2, whose impedances are 3.6 ± 0.6 kΩ and 3.8 ± 0.45 kΩ, respectively. The contact impedance of the flexible commercial electrode with pins at position 5 is 4.2 ± 0.45 kΩ. The optimal electrical conductivity and low contact impedance of the SEBS/16 wt% CNT electrode allowed to capture electrical activity from the brain.

As discussed in the previous sections, CB also improves the electrical conductivity of SEBS, but to a lesser extent than CNTs. This may result in a lower EEG signal-to-noise ratio compared to SEBS/16 wt%CNT electrode, as shown in Figs. 8 and 9. The contact impedance of polystyrene block poly(ethylene butylene) block polystyrene (SEBS)/20 wt%CB electrodes with pins at position 4 is 5.4 ± 0.9 kΩ, compared to commercial electrodes without pins at positions 1 and 2, whose impedances are 3.6 ± 0.6 kΩ and 3.8 ± 0.45 kΩ, respectively. The contact impedance of the flexible commercial electrode with pins at position 5 is 4.2 ± 0.45 kΩ.

Fig. 8 presents EEG time-domain recordings of the commercial flat dry flexible electrode at positions 1 and 2, compared to polystyrene-block-poly(ethylene butylene)-block-polystyrene (SEBS)/16 wt%CNT and SEBS/20 wt%CB at positions 3 and 4, when the subject's eyes were open and blinking. Fig. 9 presents EEG time-domain recordings of the commercial multipin dry flexible electrode at position 5, compared to SEBS/16 wt%CNT and SEBS/20 wt%CB at positions 3 and 4, when the subject's eyes were open and blinking.

The SEBS/16 wt%CNT and SEBS/20 wt%CB electrode pins help maintain stable contact with the scalp, which is essential for minimizing motion-related artifacts and ensuring a contact impedance comparable to that of flexible commercial electrodes. The SEBS/CNT electrodes, although slightly stiffer than the SEBS/CB counterparts, provide an impedance similar to that of commercial electrodes due to their low contact impedance. These electrodes may be suitable for long-term EEG recordings.

4. Discussion

This study evaluated the electrical and mechanical performance of flexible dry SEBS/CB and SEBS/CNT electrodes for EEG signal acquisition, comparing them with commercial flexible dry electrodes. The results highlight key findings regarding electrical conductivity, mechanical properties, contact impedance, and EEG signal quality.

The multipin architecture of the electrodes developed in this work improved electrode–skin contact and mechanical stability, thereby enabling reliable time-domain EEG signal acquisition. The contact impedance measured for SEBS/16 wt% CNT electrodes was 4.2 ± 0.45 kΩ, whereas SEBS/20 wt% CB electrodes with pins exhibited a slightly higher impedance of 5.4 ± 0.9 kΩ. Although SEBS/CNT multipin EEG electrodes were marginally stiffer than their SEBS/CB counterparts, both systems provided stable and reproducible electrode–skin coupling suitable for EEG measurements.

From an electrical perspective, the percolation threshold of SEBS/CB composites was approximately 12 wt%, whereas SEBS/CNT composites reached percolation at around 2 wt%. Beyond percolation, the electrical conductivity of SEBS/CB composites plateaued at ~0.01 S m^{-1} at 20 wt %, while SEBS/16 wt% CNT composites achieved a substantially higher conductivity of 1.26 S m^{-1} . These values are consistent with the work of Yang *et al.* [75], who reported percolation thresholds of 2.07 wt% for SEBS/CNT and 5.22 wt% for SEBS/CB nanocomposites using ultrasonic dispersion followed by magnetic stirring, with conductivity plateaus of

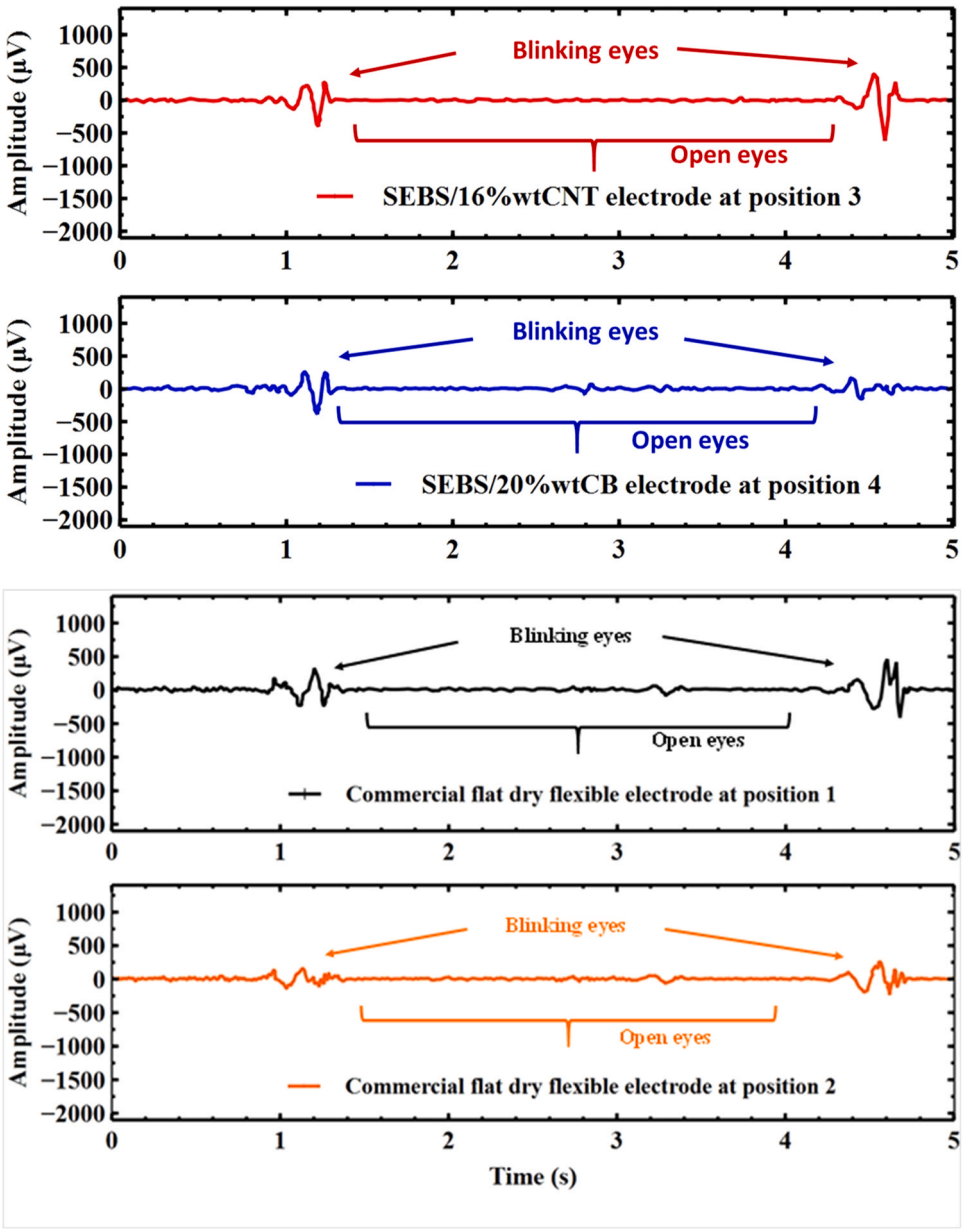

Fig. 8. Time-domain electroencephalography (EEG) recordings during eyes-open and blinking states, acquired using styrene-ethylene-butylene-styrene (SEBS)/20 wt % carbon black (CB) and styrene-ethylene-butylene-styrene (SEBS)/16 wt% carbon nanotube (CNT) composite electrodes, compared to a commercial flat dry flexible electrode.

approximately 1 S m^{-1} and 0.1 S m^{-1} , respectively. The relatively high conductivity achieved in the present electrodes is critical for efficient charge transport and reduced interfacial impedance, thereby enabling reliable detection of cortical electrical activity.

More broadly, previous studies have demonstrated that the performance of sensing and functional electrodes is strongly governed by nanocomposite architecture and interfacial charge-transfer phenomena. NiO/MWCNT-based electrodes reported in [76] exhibited reduced oxidation overpotentials, improved selectivity, and lower detection limits, highlighting the key role of CNT/oxide interfaces in facilitating charge transfer and minimizing interfacial resistance. Similarly, Mo-doped VS_2/CNT nanocomposites investigated in [77], showed increased electroactive surface area and reduced charge-transfer resistance due to synergistic interactions between CNT conductive networks and chemically doped chalcogenide phases, as confirmed by electrochemical impedance spectroscopy. Beyond electrochemical systems, CNT-based polymer nanocomposites reported in [78] exhibited unconventional electrical responses governed by filler dispersion, interfacial polarization, and percolative network formation, further underscoring the dominant influence of interfacial phenomena on macroscopic electrical behavior. In this context, the present SEBS-based CNT and CB composites follow analogous structure–property relationships, where electrode performance is primarily dictated by conductive network morphology and interfacial impedance.

The high electrical conductivity achieved in the electrodes developed in this work enabled reliable recording of brain electrical activity. Owing to their excellent intrinsic conductivity, CNT-based networks provided SEBS/CNT electrodes with low interfacial impedance, resulting in EEG waveforms comparable to those obtained using commercial flexible conductive polymer electrodes and ensuring efficient signal transmission from the scalp to the acquisition system. In contrast, carbon black, while an effective conductive filler, exhibits lower electrical conductivity than CNTs, leading to slightly higher interfacial impedance in SEBS/CB electrodes compared with both SEBS/CNT and commercial

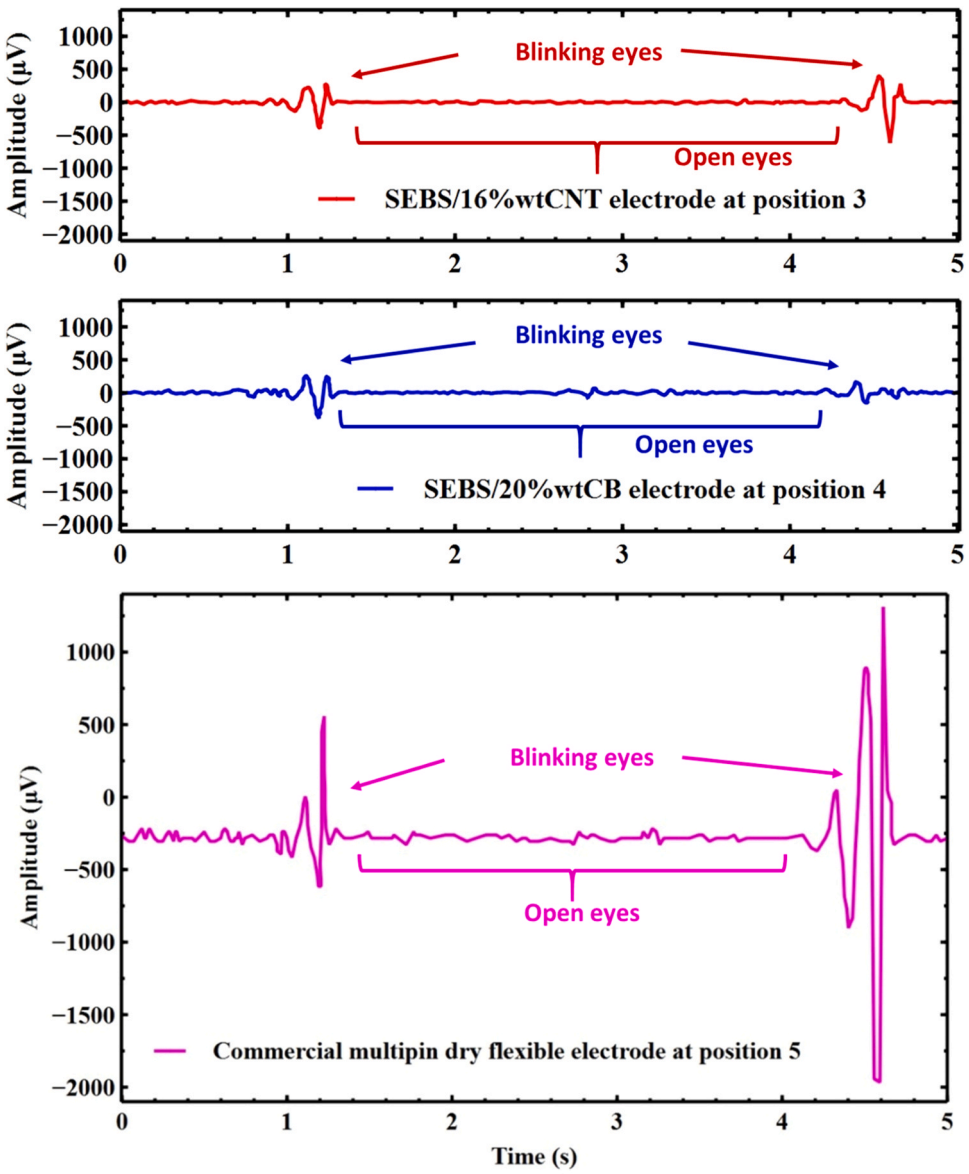

Fig. 9. Representative time-domain electroencephalography (EEG) signals during eyes-open and blinking states, demonstrating the performance of styrene-ethylene-butylene-styrene/20 wt% carbon black (SEBS/CB) composite, styrene-ethylene-butylene-styrene/16 wt% carbon nanotube (SEBS/CNT) composite, and commercial multipin electrodes. The signals illustrate the sensitivity and artifact rejection capabilities of each electrode type.

electrodes.

SEM micrographs revealed that, compared to SEBS/20 wt%CB, carbon black (CB) exhibited a greater aggregation in the matrix, whereas carbon nanotubes (CNTs) were more evenly distributed. A uniform dispersion of CB in SEBS still poses challenges, especially at high concentrations. The remaining weights obtained through TGA tests confirmed the nominal concentrations used when compounding composites. The more homogeneous dispersion of CNTs in SEBS/16 wt% CNT composites compared with the CB aggregation observed in SEBS/20 wt% CB composites is attributed to differences in filler geometry, interfacial interactions, and processing viscosity. The high aspect ratio and conjugated structure of CNTs favor uniform network formation at lower concentrations, while π–π interactions between CNTs and the styrene domains of SEBS enhance compatibility and dispersion stability. Similar π–π interfacial effects have been reported in CNT-based nanocomposites and conjugated organic frameworks, where they facilitate charge transport and structural uniformity [79–82]. In contrast, the quasi-spherical morphology and higher required loading of CB increase compound viscosity, limit shear dispersion, and promote micro-scale agglomeration [83,84]. These interfacial effects primarily explain the observed differences in dispersion and macroscopic electrical behavior, which are critical for achieving stable performance in wearable, dry EEG electrodes. Future work could explore controlled interfacial engineering or advanced characterization techniques to further elucidate the role of polymer–filler interactions on charge transport and long-term signal stability.

DMTA tests showed that the SEBS/CNT electrode is stiffer than the SEBS/CB electrode. CB and CNT offer distinct solutions for EEG applications, each having its advantages and disadvantages. CB is an economical choice with acceptable electrical conductivity at high mass concentrations, while CNTs provide acceptable electrical conductivity at low mass concentrations and high mechanical stiffness, but at a higher cost. Besides improving conductivity, CNTs increase material stiffness more than CB, potentially affecting user comfort. However, a good compromise between stiffness and flexibility would allow for stable electrodes with optimal performance. Hybrid electrodes containing SEBS, CNT, and CB could provide EEG electrodes with optimal flexibility, electrical conductivity, and contact impedance.

Recent advancements have highlighted the growing interest in hybrid nanocomposites incorporating graphene, carbon nanotubes (CNTs), and polymer matrices for the development of high-performance electrochemical sensors. For example, Bakytkarim *et al.* [85] reported a sensitive electrochemical sensor for chlorogenic acid detection based on a ternary composite consisting of multi-walled carbon nanotubes (MWCNTs), reduced graphene oxide (r-GO), and platinum nanoparticles (Pt nanoparticles (NPs)), deposited on a glassy carbon electrode (Pt/r-GO/MWCNTs/glassy carbon electrode (GCE)). The system demonstrated excellent reproducibility and sensitivity, attributed to the synergistic interaction between the high electrical conductivity of r-GO, the large surface area of MWCNTs, and the catalytic activity of Pt NPs.

Similarly, Parthasarathy [86] developed a biosensor for Escherichia coli detection using a PVA/r-GO/polyethylenimine (PEI) nanocomposite. In this case, the combination of functionalized polymers with carbon-based nanomaterials improved both electrical performance and biocompatibility, enabling a stable and selective electrochemical response suitable for biological sensing. Moreover, Biswas *et al.* [87] reviewed the potential of graphene-based hybrid nanomaterials in energy storage, particularly in supercapacitor applications. Their findings emphasize the importance of synergistic interactions between conductive fillers and polymeric hosts to achieve high surface area, efficient charge transport, and mechanical robustness. Although electrical conductivity measurements were not always reported, the observed improvements in electrochemical performance clearly demonstrate the functional benefits of hybrid material architectures. These insights support our approach in employing SEBS-based composites filled with CNTs and CB for the development of flexible dry EEG electrodes. By leveraging the mechanical flexibility and skin compatibility of SEBS, along with the high conductivity of CNTs and the low percolation threshold of CB, our hybrid electrodes achieve a balanced combination of electrical performance, mechanical stability, and low contact impedance essential features for next-generation bioelectronic interfaces.

The functioning of the developed electrodes is based on a piezoresistive sensing mechanism, in which the electrical resistance varies in response to mechanical deformation or displacement at the electrode–skin interface. This behavior resembles that of strain or displacement sensors, where signal fluctuations correspond to subtle mechanical movements. For instance, Wan *et al.* [88] demonstrated this concept in structural health monitoring by using a functionalized conductive elastomer that exhibited high sensitivity and long-term stability in detecting strain through resistance variations. In our case, the resistance changes recorded during muscle activity—such as eye blinks—can be attributed to micro-displacements and variations in contact pressure between the elastomeric pins and the scalp. These effects are closely linked to the mechanical compliance of the material and the quality of the skin–electrode contact. As such, our electrodes effectively operate as soft displacement sensors, whose performance depends on the integrity of the conductive network and the material's capacity to conform to scalp morphology under minimal applied force. In addition, Wang *et al.* [89] explored how thermo-mechanical properties influence the performance of piezo-electrets made from cyclic olefin copolymers with varying stiffness and thermal resistance. Based on the inverse relationship between the piezoelectric coefficient and the elastic modulus, their study showed that careful material selection and structural design can offset the limitations of high stiffness. These observations highlight the importance of optimizing the reinforcement ratio in elastomeric composites to ensure sufficient flexibility. Adequate flexibility is essential for maintaining stable electrode–skin contact, enabling reliable EEG signal acquisition, accommodating scalp curvature and subject motion, and improving long-term user comfort. Accordingly, this balance was a key design criterion in the development of the SEBS-based EEG electrodes.

While the current results demonstrate the potential of SEBS-based composites—particularly those reinforced with CNTs or CB—for use in flexible dry EEG electrodes, it is important to highlight that this study was deliberately limited to the characterization of material properties. Our objective was not to assess the electrodes' capacity to decode complex brain signals or validate clinical performance across different use scenarios. A more comprehensive evaluation of signal quality, stability over long-term recordings, and inter-subject reproducibility will require a dedicated clinical study involving repeated EEG acquisitions under realistic conditions. Such a study will be considered in a subsequent phase of this research. Future investigations should include comprehensive impedance characterization, including both impedance magnitude and phase angle (tan δ), performed before and after scalp cleaning to quantitatively assess the influence of scalp conditions and further validate the robustness of SEBS-based electrodes under varying conditions relevant to wearable and clinical EEG applications.

5. Conclusion

This study demonstrated the potential of SEBS-based nanocomposites as flexible dry electrodes for EEG signal acquisition. Among the tested formulations, SEBS/16 wt%CNT composite exhibited superior electrical conductivity (1.26 S/m) and the lowest contact impedance (4.2 ± 0.45 kΩ), enabling EEG signal acquisition comparable to commercial multipin electrodes. In contrast, SEBS/20 wt% CB electrodes reached a conductivity plateau of 0.01 S/m and a contact impedance of 5.4 ± 0.9 kΩ. SEM analysis confirmed a more uniform dispersion of CNTs compared to CB, which tended to agglomerate at higher concentrations. Thermogravimetric analysis validated the filler content, while DMTA results indicated that SEBS/CNT composites were stiffer than SEBS/CB ones, which may influence long-term comfort. EEG recordings from both materials revealed reliable signal detection, including blink artifacts, though SEBS/CB electrodes exhibited slightly more signal noise.

These findings suggest that SEBS/CNT composites are better suited for applications requiring high signal fidelity, whereas SEBS/CB may be favored when comfort and softness are prioritized. The ergonomic multipin design contributed to improved contact stability across the scalp, particularly in hairy areas, supporting robust EEG acquisition without conductive gel.

Future work will focus on the development of hybrid SEBS/CNT/CB electrodes to optimize the trade-off between electrical performance and mechanical compliance. Additional investigations will involve long-term user testing, analysis of motion artifacts, and performance assessment under varying physiological and environmental conditions (e.g., sweat, temperature, hair density). These efforts aim to advance the design of next-generation dry, flexible EEG systems that are biocompatible, reliable, and suitable for extended wear in real-world settings.

Author statement

The author confirms that the work presented in this manuscript is original, has not been published elsewhere, and is not under consideration for publication in any other journal. All data, analyses, and conclusions are the result of the author's own research, conducted in accordance with ethical guidelines. The author has read and approved the final version of the manuscript and agrees to be accountable for all aspects of the work.

Ethical statement

All experimental procedures involving human participants were conducted in accordance with the ethical standards of the institutional research committee. The study protocol was reviewed and approved by the Research Ethics Committee of the École de technologie supérieure under approval number H20230504. Informed consent was obtained from all individual participants included in the study.

CRediT authorship contribution statement

Ilyass Tabiai: Writing – review & editing, Supervision, Funding acquisition, Conceptualization. **George Gnonhoue:** Writing – review & editing, Writing – original draft, Validation, Methodology, Investigation, Formal analysis, Conceptualization. **Jérémie Voix:** Writing – review & editing, Validation, Supervision, Funding acquisition, Conceptualization. **Éric David:** Writing – review & editing, Supervision, Funding acquisition, Conceptualization.

Declaration of Competing Interest

The authors declare that they have no known competing financial interests or personal relationships that could have appeared to influence the work reported in this paper.

Acknowledgements

The authors would like to acknowledge the financial support received from NSERC Alliance (ALLRP 566678–2021), MITACS IT26677 (SUBV-2021–168), and PROMPT (#164_Voix-EERS 2021.06) for the ÉTS-EERS Industrial Research Chair in Ear Technologies, sponsored by EERS Global Technologies Inc.

Data availability

The data that has been used is confidential.

References

[1] L. Xiong, N. Li, Y. Luo, L. Chen, Sustainable development of electroencephalography materials and technology, SusMat 4 (2024) e195, https://doi.org/10.1002/sus2.195.
[2] A. Palumbo, V. Gramigna, B. Calabrese, N. Ielpo, A. Demeco, A wearable device-based system: the potential role in real-time and remote EEG monitoring, fbt (2024), https://doi.org/10.18502/fbt.v11i3.15882.
[3] J. Huang, C. Wang, W. Zhao, A. Grau, X. Xue, F. Zhang, LTDNet-EEG: a lightweight network of portable/wearable devices for real-time EEG signal denoising, IEEE Trans. Consum. Electron (2024) 1, https://doi.org/10.1109/TCE.2024.3412774.
[4] G. Di Flumeri, P. Aricò, G. Borghini, N. Sciaraffa, A. Di Florio, F. Babiloni, The dry revolution: evaluation of three different EEG dry electrode types in terms of signal spectral features, mental states classification and usability, Sensors 19 (2019) 1365, https://doi.org/10.3390/s19061365.
[5] G. Petrossian, P. Kateb, F. Miquet-Westphal, F. Cicoira, Advances in electrode materials for scalp, forehead, and ear EEG: a mini-review, ACS Appl. Bio Mater. 6 (2023) 3019–3032, https://doi.org/10.1021/acsabm.3c00322.
[6] H.-L. Peng, J.-Q. Liu, H.-C. Tian, B. Xu, Y.-Z. Dong, B. Yang, X. Chen, C.-S. Yang, Flexible dry electrode based on carbon nanotube/polymer hybrid micropillars for biopotential recording, Sens. Actuators A Phys. 235 (2015) 48–56, https://doi.org/10.1016/j.sna.2015.09.024.
[7] M. Zeydabadinezhad, J. Jowers, D. Buhl, B. Cabaniss, B. Mahmoudi, A personalized earbud for non-invasive long-term EEG monitoring, J. Neural Eng. 21 (2024) 026026, https://doi.org/10.1088/1741-2552/ad33af.
[8] S. Lin, J. Liu, W. Li, D. Wang, Y. Huang, C. Jia, Z. Li, M. Murtaza, H. Wang, J. Song, et al., A flexible, robust, and gel-free electroencephalogram electrode for noninvasive brain-computer interfaces, Nano Lett. 19 (2019) 6853–6861, https://doi.org/10.1021/acs.nanolett.9b02019.
[9] G. Li, S. Wang, Y.Y. Duan, Towards conductive-gel-free electrodes: understanding the wet electrode, semi-dry electrode and dry electrode-skin interface impedance using electrochemical impedance spectroscopy fitting, Sens. Actuators B Chem. 277 (2018) 250–260, https://doi.org/10.1016/j.snb.2018.08.155.
[10] P. Li, J. Huang, M. Li, H. Li, Evaluation of flexible multi-claw and multi-channel semi-dry electrodes for evoked electroencephalography recording, Sens. Actuators A Phys. 340 (2022) 113547, https://doi.org/10.1016/j.sna.2022.113547.
[11] G. Li, N. Chen, T. Xu, Y. Zhang, Flexible Fe3 +-doped gelatin/poly(Acrylate-Co-Acrylamide) conductive hydrogels for biopotential acquisition, salt recognition, and supercapacitors, Sens. Actuators A Phys. 387 (2025) 116425, https://doi.org/10.1016/j.sna.2025.116425.
[12] G. Li, Y. Liu, Y. Chen, M. Li, J. Song, K. Li, Y. Zhang, L. Hu, X. Qi, X. Wan, et al., Polyvinyl alcohol/polyacrylamide double-network hydrogel-based semi-dry electrodes for robust electroencephalography recording at hairy scalp for noninvasive brain–computer interfaces, J. Neural Eng. 20 (2023) 026017, https://doi.org/10.1088/1741-2552/acc098.
[13] G. Li, S. Wang, M. Li, Y.Y. Duan, Towards real-life EEG applications: novel superporous hydrogel-based semi-dry EEG electrodes enabling automatically 'charge–discharge' electrolyte, J. Neural Eng. 18 (2021) 046016, https://doi.org/10.1088/1741-2552/abeeab.
[14] G.-L. Li, J.-T. Wu, Y.-H. Xia, Q.-G. He, H.-G. Jin, Review of semi-dry electrodes for EEG recording, J. Neural Eng. 17 (2020) 051004, https://doi.org/10.1088/1741-2552/abbd50.
[15] M.P. Sidheekha, A. Shabeeba, L. Rajan, M.S. Thayyil, Y.A. Ismail, Conducting polymer/hydrogel hybrid free-standing electrodes for flexible supercapacitors capable of self-sensing working conditions: large-scale fabrication through facile and low-cost route, Eng. Sci. (2023), https://doi.org/10.30919/es890.
[16] A. Veronica, H.Y.Y. Nyein, I.-M. Hsing, Ionogels and eutectogels for stable and long-term EEG and EMG signal acquisition, Mater. Futures 3 (2024) 033501, https://doi.org/10.1088/2752-5724/ad5c84.
[17] F. Wang, M. Ma, R. Fu, X. Zhang, EEG-based detection of driving fatigue using a novel electrode, Sens. Actuators A Phys. 365 (2024) 114895, https://doi.org/10.1016/j.sna.2023.114895.
[18] M. Dadjou, S. Bakhtiyari, A. Jahanshahi, R. Bagherzadeh, Towards seamless conformable and comfortable wearable electronics: polyimide-supported dry electrodes integrated in knitted fabrics, Sens. Actuators A Phys. 376 (2024) 115613, https://doi.org/10.1016/j.sna.2024.115613.
[19] P. Van Der Heijden, C. Gilbert, S. Jafari, M.A. Lucchini, Multi-channel soft dry electrodes for electrocardiography acquisition in the ear region, Sensors 24 (2024) 420, https://doi.org/10.3390/s24020420.
[20] Y. Peng, J. Dong, Y. Zhang, Y. Zhang, J. Long, J. Sun, T. Liu, Y. Huang, Thermally comfortable epidermal bioelectrodes based on ultrastretchable and passive radiative cooling e-textiles, Nano Energy 120 (2024) 109143, https://doi.org/10.1016/j.nanoen.2023.109143.
[21] O. Lee, H. Lee, Development and printing of three-dimensional electrodes for the high body adhesion of smart wear, Fash. Text. 11 (2024) 29, https://doi.org/10.1186/s40691-024-00392-w.
[22] K. Gao, L. Li, B. Ji, N. Wu, Pin-shaped Ag/AgCl fabric electrode coated with hydrogel for EEG recording in hairy areas, IEEE Sens. J. 24 (2024) 25316–25327, https://doi.org/10.1109/JSEN.2024.3426268.
[23] R. Kaveh, C. Schwendeman, L. Pu, A.C. Arias, R. Muller, Wireless ear EEG to monitor drowsiness, Nat. Commun. 15 (2024) 6520, https://doi.org/10.1038/s41467-024-48682-7.
[24] L. Xing, A.J. Casson, 3D-printed, directly conductive and flexible electrodes for personalized electroencephalography, Sens. Actuators A Phys. 349 (2023) 114062, https://doi.org/10.1016/j.sna.2022.114062.
[25] S. Lin, J. Jiang, K. Huang, L. Li, X. He, P. Du, Y. Wu, J. Liu, X. Li, Z. Huang, et al., Advanced electrode technologies for noninvasive brain–computer interfaces, ACS Nano 17 (2023) 24487–24513, https://doi.org/10.1021/acsnano.3c06781.
[26] Z. Shi, B. Jiang, S. Liang, J. Zhang, D. Suo, J. Wu, D. Chen, G. Pei, T. Yan, Claw-shaped flexible and low-impedance conductive polymer electrodes for EEG recordings: anemone dry electrode, Sci. China Technol. Sci. 66 (2023) 255–266, https://doi.org/10.1007/s11431-022-2231-3.
[27] R.B. Damalerio, R. Lim, Y. Gao, T.-T. Zhang, M.-Y. Cheng, Development of low-contact-impedance dry electrodes for electroencephalogram signal acquisition, Sensors 23 (2023) 4453, https://doi.org/10.3390/s23094453.
[28] L. Xing, A.J. Casson, Directly Conductive, Flexible, 3D Printed, EEG Electrodes. In Proceedings of the 2022 IEEE International Conference on Flexible and Printable Sensors and Systems (FLEPS), IEEE, Vienna, Austria, 2022, pp. 1–4.
[29] I.F. Warsito, M. Komosar, M.A. Bernhard, P. Fiedler, J. Haueisen, Flower electrodes for comfortable dry electroencephalography, Sci. Rep. 13 (2023) 16589, https://doi.org/10.1038/s41598-023-42732-8.
[30] J. Haueisen, P. Fiedler, A. Bernhardt, R. Gonçalves, C. Fonseca, Novel dry electrode EEG headbands for home use: comparing performance and comfort, Curr. Dir. Biomed. Eng. 6 (2020) 139–142, https://doi.org/10.1515/cdbme-2020-3036.
[31] J.J.A. Heijs, R.J. Havelaar, P. Fiedler, R.J.A. Van Wezel, T. Heida, Validation of soft multipin dry EEG electrodes, Sensors 21 (2021) 6827, https://doi.org/10.3390/s21206827.
[32] Q. Liu, L. Yang, Z. Zhang, H. Yang, Y. Zhang, J. Wu, The feature, performance, and prospect of advanced electrodes for electroencephalogram, Biosensors 13 (2023) 101, https://doi.org/10.3390/bios13010101.
[33] P. Fiedler, U. Graichen, E. Zimmer, J. Haueisen, Simultaneous dry and gel-based high-density electroencephalography recordings, Sensors 23 (2023) 9745, https://doi.org/10.3390/s23249745.
[34] A.D.-A. Abdullah, A.Q. Al-Neami, Performance Evaluation of a New Dry-Contact Electrode for EEG Measurement. In Proceedings of the 2021 IEEE International Biomedical Instrumentation and Technology Conference (IBITeC), IEEE, Yogyakarta, Indonesia, 2021, pp. 119–123.
[35] K. Chen, Z. Li, J. Guo, X. Yang, B. Guo, H. Shen, A flexible capacitive pressure sensor based on thermoplastic polyurethane porous films by non-solvent induced phase separation, IEEE Sens. J. 24 (2024) 12217–12224, https://doi.org/10.1109/JSEN.2024.3372587.
[36] X. Zhao, J. Li, M. Jiang, W. Zhai, K. Dai, C. Liu, C. Shen, Flexible strain sensor based on CNTs/CB/TPU conductive fibrous film with wide sensing range and high sensitivity for human biological signal acquisition, Polymer 302 (2024) 127049, https://doi.org/10.1016/j.polymer.2024.127049.
[37] W. Hong, X. Guo, T. Zhang, S. Mu, F. Wu, Z. Yan, H. Zhang, X. Li, A. Zhang, J. Wang, et al., Flexible strain sensor based on nickel microparticles/carbon black microspheres/polydimethylsiloxane conductive composites for human motion detection, ACS Appl. Mater. Interfaces 16 (2024) 32702–32712, https://doi.org/10.1021/acsami.4c04830.
[38] J. Wang, T. Wang, H. Liu, K. Wang, K. Moses, Z. Feng, P. Li, W. Huang, Flexible electrodes for brain–computer interface system, Adv. Mater. 35 (2023) 2211012, https://doi.org/10.1002/adma.202211012.

[39] J. Lozano, B. Stoeber, Microspike Array Electrode with Flexible Backing for Biosignal Monitoring. In Proceedings of the 2019 IEEE SENSORS, IEEE: Montreal, QC, Canada, 2019, pp. 1–4.
[40] Y. Xiao, M. Wang, Y. Li, Z. Sun, Z. Liu, L. He, R. Liu, High-adhesive flexible electrodes and their manufacture: a review, Micromachines 12 (2021) 1505, https://doi.org/10.3390/mi12121505.
[41] Y. Fu, J. Zhao, Y. Dong, X. Wang, Dry electrodes for human bioelectrical signal monitoring, Sensors 20 (2020) 3651, https://doi.org/10.3390/s20133651.
[42] B.-S. Lin, H.-A. Wang, Y.-K. Huang, Y.-L. Wang, B.-S. Lin, Design of SSVEP enhancement-based brain computer interface, IEEE Sens. J. 21 (2021) 14330–14338, https://doi.org/10.1109/JSEN.2020.3033470.
[43] P. Fiedler, P. Pedrosa, S. Griebel, C. Fonseca, F. Vaz, E. Supriyanto, F. Zanow, J. Haueisen, Novel multipin electrode cap system for dry electroencephalography, Brain Topogr. 28 (2015) 647–656, https://doi.org/10.1007/s10548-015-0435-5.
[44] Z. Wang, Y. Ding, W. Yuan, H. Chen, W. Chen, C. Chen, Active claw-shaped dry electrodes for EEG measurement in hair areas, Bioengineering 11 (2024) 276, https://doi.org/10.3390/bioengineering11030276.
[45] L. Xing, A.J. Casson, 3D-printed, directly conductive and flexible electrodes for personalized electroencephalography, Sens. Actuators A Phys. 349 (2023) 114062, https://doi.org/10.1016/j.sna.2022.114062.
[46] P.S. Das, S.H. Park, K.Y. Baik, J.W. Lee, J.Y. Park, Thermally reduced graphene oxide-nylon membrane based epidermal sensor using vacuum filtration for wearable electrophysiological signals and human motion monitoring, Carbon 158 (2020) 386–393, https://doi.org/10.1016/j.carbon.2019.11.001.
[47] J. Oh, K.-W. Nam, W.-J. Kim, B.-H. Kang, S.-H. Park, Flexible dry electrode based on a wrinkled surface that uses carbon nanotube/polymer composites for recording electroencephalograms, Materials 17 (2024) 668, https://doi.org/10.3390/ma17030668.
[48] P. Sharma, S. Baloda, D. Verma, V. Janyani, R. Sharma, N. Gupta, Multiwall carbon nanotube/polydimethylsiloxane composites-based dry electrodes for bio-signal detection, IEEE Flex. Electron 3 (2024) 108–114, https://doi.org/10.1109/JFLEX.2024.3367648.
[49] L.-F. Wang, J.-Q. Liu, B. Yang, C.-S. Yang, PDMS-based low cost flexible dry electrode for long-term EEG measurement, IEEE Sens. J. 12 (2012) 2898–2904, https://doi.org/10.1109/JSEN.2012.2204339.
[50] M. Robertson, A. Guillen-Obando, A. Barbour, P. Smith, A. Griffin, Z. Qiang, Direct synthesis of ordered mesoporous materials from thermoplastic elastomers, Nat. Commun. 14 (2023) 639, https://doi.org/10.1038/s41467-023-36362-x.
[51] Y. Xu, B. Sun, Y. Ling, Q. Fei, Z. Chen, X. Li, P. Guo, N. Jeon, S. Goswami, Y. Liao, et al., Multiscale porous elastomer substrates for multifunctional on-skin electronics with passive-cooling capabilities, Proc. Natl. Acad. Sci. U. S. A. 117 (2020) 205–213, https://doi.org/10.1073/pnas.1917762116.
[52] M. Xu, J. Li, J. Ren, J. Wang, L. Xu, W. Wang, S. Sun, H. Li, J. Zhang, J. Wu, Superhydrophobic and recyclable passive daytime radiative cooling fabric prepared via electrospinning, Chem. Eng. J. 509 (2025) 161274, https://doi.org/10.1016/j.cej.2025.161274.
[53] W. Zhong, Y. Chen, J. Sun, X. Wang, D. Hu, L. Zhao, Preparation of SEBS foam for new-generation sports protection and monitoring by microwave selective sintering, Chem. Eng. J. 515 (2025) 163494, https://doi.org/10.1016/j.cej.2025.163494.
[54] R. Wang, L. Geng, X. Zhang, G. Liang, J. Zhao, C. Liu, Synthesis of flexible form stable phase change materials with in-situ formed porous TiO2 for personal thermal management, Chem. Eng. J. 505 (2025) 159592, https://doi.org/10.1016/j.cej.2025.159592.
[55] R. Bidiyasar, R. Kumar, N. Jakhar, A critical review of polymer support-based shape-stabilized phase change materials for thermal energy storage applications, Energy Storage 6 (2024) e639, https://doi.org/10.1002/est2.639.
[56] E. Habibzadeh Tonekabony Shad, M. Molinas, T. Ytterdal, Impedance and noise of passive and active dry EEG electrodes: a review, IEEE Sens. J. 20 (2020) 14565–14577, https://doi.org/10.1109/JSEN.2020.3012394.
[57] L. Yang, Q. Liu, Z. Zhang, L. Gan, Y. Zhang, J. Wu, Materials for dry electrodes for the electroencephalography: advances, challenges, perspectives, Adv. Mater. Technol. (2021) 2100612, https://doi.org/10.1002/admt.202100612.
[58] N.V. de Camp, G. Kalinka, J. Bergeler, Light-cured polymer electrodes for non-invasive EEG recordings, Sci. Rep. 8 (2018) 14041, https://doi.org/10.1038/s41598-018-32304-6.
[59] P.S. Das, S.H. Park, K.Y. Baik, J.W. Lee, J.Y. Park, Thermally reduced graphene oxide-nylon membrane based epidermal sensor using vacuum filtration for wearable electrophysiological signals and human motion monitoring, Carbon 158 (2020) 386–393, https://doi.org/10.1016/j.carbon.2019.11.001.
[60] Y. Fu, J. Zhao, Y. Dong, X. Wang, Dry electrodes for human bioelectrical signal monitoring, Sensors 20 (2020) 3651, https://doi.org/10.3390/s20133651.
[61] E. Tekay, B. Aybakan, V.U. Aslan, 4D printable maleated poly(Styrene-b-Ethylene/Butylene-b-Styrene) / Poly(Ethylene-Co-Vinyl Acetate) thermoplastic elastomer blends; effects of blend composition on shape memory and mechanical properties, Addit. Manuf. 78 (2023) 103870, https://doi.org/10.1016/j.addma.2023.103870.
[62] M. Liu, Y. Sheng, C. Huang, Y. Zhou, L. Jiang, M. Tian, S. Chen, S. Jerrams, F. Zhou, J. Yu, Highly stretchable and sensitive SBS/Gr/CNTs fibers with hierarchical structure for strain sensors, Composites Part A Applied Science Manufacturing 164 (2023) 107296, https://doi.org/10.1016/j.compositesa.2022.107296.
[63] B. Zhou, Z. Liu, C. Li, L. Li, X. Zhang, Y. Sheng, Y. Zhou, L. Jiang, M. Tian, S. Chen, Fabrication of ultrasensitive and flexible strain sensor based on multi-wall carbon nanotubes coated electrospun styrene-ethylene-butylene-styrene block copolymer fibrous tubes, Eur. Polym. J. 178 (2022) 111501, https://doi.org/10.1016/j.eurpolymj.2022.111501.
[64] M.S. Cetin, H.A. Karahan Toprakci, Flexible electronics from hybrid nanocomposites and their application as piezoresistive strain sensors, Composites Part B Engineering 224 (2021) 109199, https://doi.org/10.1016/j.compositesb.2021.109199.
[65] E. Tekay, Preparation and characterization of electro-active shape memory PCL/SEBS-g-MA/MWCNT nanocomposites, Polymer 209 (2020) 122989, https://doi.org/10.1016/j.polymer.2020.122989.
[66] X. Wang, S. Meng, M. Tebyetekerwa, Y. Li, J. Pionteck, B. Sun, Z. Qin, M. Zhu, Highly sensitive and stretchable piezoresistive strain sensor based on conductive poly(styrene-butadiene-styrene)/few layer graphene composite fiber, Composites Part A Applied Science Manufacturing 105 (2018) 291–299, https://doi.org/10.1016/j.compositesa.2017.11.027.
[67] X. Yang, L. Sun, C. Zhang, B. Huang, Y. Chu, B. Zhan, Modulating the sensing behaviors of poly(styrene-ethylene-butylene-styrene)/carbon nanotubes with low-dimensional fillers for large deformation sensors, Composites Part B Engineering 160 (2019) 605–614, https://doi.org/10.1016/j.compositesb.2018.12.119.
[68] M.N. Alam, V. Kumar, D. Lee, S. Park, Styrene–butadiene rubber-based nanocomposites toughened by carbon nanotubes for wide and linear electromechanical sensing applications, Polym. Compos. 45 (2024) 2485–2499, https://doi.org/10.1002/pc.27934.
[69] M.N. Alam, V. Kumar, D.-J. Lee, J. Choi, Magnetically active response of acrylonitrile-butadiene-rubber-based magnetorheological elastomers with different types of iron fillers and their hybrid, Compos. Commun. 24 (2021) 100657, https://doi.org/10.1016/j.coco.2021.100657.
[70] S.R. Sinha, L. Sullivan, D. Sabau, D. San-Juan, K.E. Dombrowski, J.J. Halford, A. J. Hani, F.W. Drislane, M.M. Stecker, American clinical neurophysiology society guideline 1: minimum technical requirements for performing clinical electroencephalography, J. Clin. Neurophysiol. 33 (2016) 303–307, https://doi.org/10.1097/WNP.0000000000000308.
[71] A. Kausar, Poly(vinylacetate)cyanomethyl diphenylcarbamodthioate/ poly(vinyl acetate)/carbon black composite-based sensor, Int. J. Instrum. Sci. (2016), https://doi.org/10.5923/j.instrument.20160502.01.
[72] H. Lin, J. Wang, W. Cao, H. Wang, K. Rui, Y. Yan, J. Zhu, Hierarchical conducting networks constructed as resistive strain sensors for personal healthcare monitoring and robotic arm control, Chem. Eng. J. 490 (2024) 151840, https://doi.org/10.1016/j.cej.2024.151840.
[73] M.S. Cetin, H.A. Karahan Toprakci, Flexible electronics from hybrid nanocomposites and their application as piezoresistive strain sensors, Compos. Part B Eng. 224 (2021) 109199, https://doi.org/10.1016/j.compositesb.2021.109199.
[74] A.N. Kouediatouka, Q. Liu, F.J. Mawignon, W. Wang, J. Wang, C. Ruan, K.F.H. Yeo, G. Dong, Sensing characterization of an amorphous PDMS/ecoflex blend composites with an improved interfacial bonding and rubbing performance, Appl. Surf. Sci. 635 (2023) 157675, https://doi.org/10.1016/j.apsusc.2023.157675.
[75] X. Yang, L. Sun, C. Zhang, B. Huang, Y. Chu, B. Zhan, Modulating the sensing behaviors of poly(styrene-ethylene-butylene-styrene)/carbon nanotubes with low-dimensional fillers for large deformation sensors, Compos. Part B Eng. 160 (2019) 605–614, https://doi.org/10.1016/j.compositesb.2018.12.119.
[76] M.R. Shahmiri, A. Bahari, H. Karimi-Maleh, R. Hosseinzadeh, N. Mirnia, Ethynylferrocene–NiO/MWCNT nanocomposite modified carbon paste electrode as a novel voltammetric sensor for simultaneous determination of glutathione and acetaminophen, Sens. Actuators B Chem. 177 (2013) 70–77, https://doi.org/10.1016/j.snb.2012.10.098.
[77] N. Moradbeigi, A. Bahari, S. Ghasemi, Effect of molybdenum doping on the catalytic activity of VS_2 /CNT for the oxygen reduction reaction in alkaline media, N. J. Chem. 47 (2023) 1291–1298, https://doi.org/10.1039/D2NJ04721G.
[78] H.R. Litkohi, A. Bahari, M.P. Gatabi, Pt/Fe/Ni decorated CVD grown CNTs on carbon paper as electrocatalytic electrodes in polymer fuel cells: an investigation on H2 gas on the growth of CNTs and reduction of electrocatalysts, Diam. Relat. Mater. 119 (2021) 108534, https://doi.org/10.1016/j.diamond.2021.108534.
[79] D. Yan, L. Song, F. Kang, X. Mo, Y. Lv, J. Sun, H. Tang, X. Zhou, Q. Zhang, *In Situ* growth of covalent organic frameworks on carbon nanotubes for high-performance potassium-ion batteries, Angew. Chem. 137 (2025) e202422851, https://doi.org/10.1002/ange.202422851.
[80] J. Zhu, J. Li, A. Duan, H. Wang, Boosting a high-performance desalination in flow-electrode capacitive deionization (FCDI): unraveling the role of dynamic $\pi - \pi$ stacking between a current collector and flow-electrode on enhancing charge transfer, Desalination 601 (2025) 118568, https://doi.org/10.1016/j.desal.2025.118568.
[81] Y. Qin, C. Zhang, Y. Wang, P. She, W. Wong, Electrostatic attraction-driven assembly of non-noble metallo-supramolecular polymers with single-walled carbon nanotubes for boosting photocatalytic hydrogen evolution, Carbon Energy 7 (2025) e70003, https://doi.org/10.1002/cey2.70003.
[82] L. Jing, P. Li, Z. Li, D. Ma, J. Hu, Influence of π–π interactions on organic photocatalytic materials and their performance, Chem. Soc. Rev. 54 (2025) 2054–2090, https://doi.org/10.1039/D4CS00029C.
[83] M. Atif, R. Bongiovanni, M. Giorcelli, E. Celasco, A. Tagliaferro, Modification and characterization of carbon black with mercaptopropyltrimethoxysilane, Appl. Surf. Sci. 286 (2013) 142–148, https://doi.org/10.1016/j.apsusc.2013.09.037.
[84] J.C. Gómez Martín, O. Muñoz, J. Martikainen, D. Guirado, I. Tanarro, R.J. Peláez, B. Maté, M. Jiménez-Redondo, V.J. Herrero, M. Peiteado, et al., Experimental phase function and degree of linear polarization of light scattered by hydrogenated amorphous carbon circumstellar dust analogs, ApJS 270 (2024) 2, https://doi.org/10.3847/1538-4365/ad0379.
[85] Y. Bakytkarim, S. Tursynbolat, Mukatayeva Zh.S, Tileuberdi Ye, N.A. Shadin, Assirbayeva Zh.M, L.S. Wang, L.A. Zhussupova, Z. Toktarbay, High-sensitivity electrochemical detection of chlorogenic acid based on Pt@r-GO@MWCNTs ternary nanocomposites modified electrodes, Eng. Sci. (2024), https://doi.org/10.30919/es1178.

[86] P. P, Electrochemical detection of uropathogenic escherichia coli using PVA/R-GO/PEI modified nanocomposite electrode, Eng. Sci. (2023), https://doi.org/10.30919/es903.
[87] S. Biswas, A. Biswas, K. Sen, Graphene based hybrid nanocomposite materials as sustainable energy resource: synthesis to application as supercapacitors, ES Chem. Sustain. (2025), https://doi.org/10.30919/escs1581.
[88] B. Wan, Y. Yang, R. Guo, X. Yu, Functionalised conductive elastomers for strain monitoring of seismic isolation bearings: experiments and molecular simulations, Eng. Sci. (2025), https://doi.org/10.30919/es1479.
[89] H. Wang, X. Wang, Y. Li, Z. Liu, M.F. Ahmed, X. Zhang, C. Zeng, Piezoelectrets from cyclic olefin copolymers with different mechanical and thermomechanical properties: a comparative study, Eng. Sci. (2023), https://doi.org/10.30919/es8d810.

George Gnonhoue is a Ph.D. student in Mechanical Engineering at the École de technologie supérieure (ÉTS), where his research focuses on advanced polymer composites and their applications in bioelectronics and structural health monitoring. He also holds two master's degrees: one in Electrical Engineering, specializing in high-voltage direct current (HVDC) systems, and another in Materials Science with an emphasis on dielectric film capacitor characterization. He is currently working as a Materials and Process Engineer at Hutchinson Canada, contributing to the development and optimization of advanced materials for aerospace applications. His research interests include flexible and wearable sensors, conductive polymer nanocomposites, EEG electrode design, and multifunctional materials for aerospace and biomedical applications. George Gnonhoue has authored several peer-reviewed publications and has been actively involved in collaborative projects with both academic and industrial partners.